



Discover Generics

Cost-Effective CT & MRI Contrast Agents

**FRESENIUS
KABI**

[WATCH VIDEO](#)

AJNR

This information is current as
of June 22, 2025.

Spinal Compliance Curves: Preliminary Experience with a New Tool for Evaluating Suspected CSF Venous Fistulas on CT Myelography in Patients with Spontaneous Intracranial Hypotension

M.T. Caton, Jr, B. Laguna, K.A. Soderlund, W.P. Dillon and
V.N. Shah

AJNR Am J Neuroradiol 2021, 42 (5) 986-992

doi: <https://doi.org/10.3174/ajnr.A7018>

<http://www.ajnr.org/content/42/5/986>

Spinal Compliance Curves: Preliminary Experience with a New Tool for Evaluating Suspected CSF Venous Fistulas on CT Myelography in Patients with Spontaneous Intracranial Hypotension

M.T. Caton Jr, B. Laguna, K.A. Soderlund, W.P. Dillon, and V.N. Shah

ABSTRACT

BACKGROUND AND PURPOSE: Craniospinal space compliance reflects the distensibility of the spinal and intracranial CSF spaces as a system. Craniospinal space compliance has been studied in intracranial pathologies, but data are limited in assessing it in spinal CSF leak. This study describes a method to estimate craniospinal space compliance using saline infusion during CT myelography and explores the use of craniospinal space compliance and pressure-volume curves in patients with suspected cerebrospinal-venous fistula.

MATERIALS AND METHODS: Patients with suspected cerebrospinal-venous fistula underwent dynamic CT myelography. During the procedure, 1- to 5-mL boluses of saline were infused, and incremental changes in CSF pressure were recorded. These data were used to plot craniospinal space compliance curves. We calculated 3 quantitative craniospinal space compliance parameters: overall compliance, compliance at opening pressure, and the pressure volume index. These variables were compared between patients with confirmed cerebrospinal-venous fistula and those with no confirmed source of CSF leak.

RESULTS: Thirty-four CT myelograms in 22 patients were analyzed. Eight of 22 (36.4%) patients had confirmed cerebrospinal-venous fistulas. Bolus infusion was well-tolerated with no complications and transient headache in 2/34 (5.8%). Patients with confirmed cerebrospinal-venous fistulas had higher compliance at opening pressure and overall compliance (2.6 versus 1.8 mL/cm H₂O, $P < .01$). There was no difference in the pressure volume index (77.5 versus 54.3 mL, $P = .13$) between groups.

CONCLUSIONS: A method of deriving craniospinal space compliance curves using saline intrathecal infusion is described. Preliminary analysis of craniospinal space compliance curves provides qualitative and quantitative information about pressure-volume dynamics and may serve as a diagnostic tool in patients with known or suspected cerebrospinal-venous fistulas.

ABBREVIATIONS: C_{op} = compliance at opening pressure; CSC = cerebrospinal space compliance; CTM = CT myelography; CVF = cerebrospinal-venous fistula; PVI = pressure-volume index; SIH = spontaneous intracranial hypotension

Spontaneous intracranial hypotension (SIH) is a debilitating-but-potentially curable syndrome caused by spinal CSF leakage. CSF-venous fistulas (CVFs) are a recently discovered cause of SIH and should be suspected in patients with persistent clinical and brain imaging features of SIH who lack extradural CSF on CT or MR myelography.¹ CVFs are challenging to diagnose and may be position-, volume-, and pressure-dependent; therefore, the true prevalence is likely underestimated.²⁻⁴ Dynamic CT myelography (CTM) and digital subtraction fluoroscopy can facilitate diagnosis,

but the sensitivity of these techniques remains modest.⁵ The pathophysiology of CVF remains poorly understood but is closely tied to the pressure-volume dynamics of the craniospinal axis.² Knowledge of patient-specific CSF pressure-volume dynamics may, therefore, aid in CVF diagnosis and improve our understanding of CVF pathogenesis.

Craniospinal space compliance (CSC) reflects the distensibility of the CSF system as a change in volume relative to a change in pressure.⁶ Building on the Monro-Kellie doctrine, work by Shapiro et al⁷ showed that CSC forms an exponential rather than linear curve. They defined the pressure-volume index (PVI) as a reproducible measure of CSC accounting for this nonlinear relationship, mathematically representing the infusion volume necessary to raise CSF pressure by an order of magnitude.⁷

Later work showed that the PVI can be reliably calculated using bolus-response measurements as opposed to steady-state infusion, more easily performed during routine myelography.⁸

Received August 24, 2020; accepted after revision November 19.

From the Department of Radiology and Biomedical Imaging, Neuroradiology Section, University of California San Francisco, San Francisco, California.

Paper previously presented as a digital poster at: Annual Meeting of the American Society of Neuroradiology, May 30 to June 4, 2020; Virtual.

Please address correspondence to M. Travis Caton, Jr, MD, 505 Parnassus Ave, Room L349, San Francisco, CA 94143; e-mail: michael.caton2@ucsf.edu; @traviscaton

<http://dx.doi.org/10.3174/ajnr.A7018>

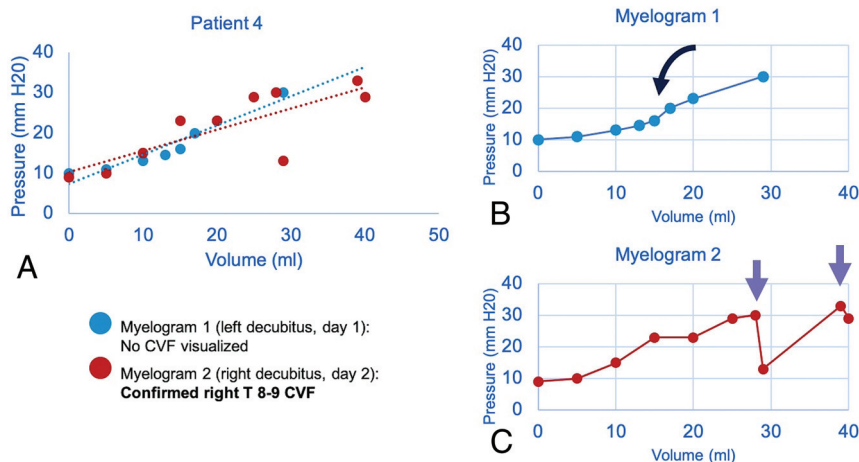


FIG 1. Sample craniospinal compliance curves in a 51-year-old man confirmed to have CVF at operation. Combined plot of 2 CTMs with *dashed lines* showing a linear approximation of compliance (A). Initial nondiagnostic CTM (B) shows a roughly sigmoid pattern with an inflection point seen after a ~15-mL normal saline bolus was administered (*black curved arrow*). Repeat CTM with more aggressive positive-pressure augmentation shows an abrupt loss of pressure (*purple arrows*) after infusion volume of 27 mL of normal saline (C). The CVF became apparent only after pressure was increased beyond this threshold point.

Recent work and our experience indicate that CVF detection is improved with CSF pressure augmentation, which can be achieved with patient positioning, respiratory phase variation, or fluid infusion to the thecal sac.^{3,9-11} Building on prior studies of CSF pressure-volume dynamics using intrathecal CSF infusion in healthy subjects^{12,13} and in pathologic states such as normal-pressure hydrocephalus,¹⁴ we aimed to present our preliminary experience in estimating CSF compliance and PVI using bolus CSF pressure augmentation in patients with SIH suspected of having a CVF.

MATERIALS AND METHODS

In this retrospective case series, we reviewed clinical and imaging records of adult patients with clinical and brain imaging features of SIH suspected of having a CVF from 2015 to 2019 at a single, tertiary referral center. Inclusion criteria were as follows: 1) All patients underwent an initial work-up comprising brain MR imaging and either spine MR imaging or conventional myelography, 2) all patients met the International Classification of Headache Disorders-3 criteria for SIH, and 3) each patient had at least 2 pressure-volume point recordings. Patients with SIH who did not meet these criteria or had confirmation of a non-CVF cause of SIH were excluded. Our institutional CSF leak spine imaging protocol comprises fat-saturated, T2-weighted images of the whole spine in sagittal and coronal planes. In each case, there were findings of SIH on brain MR imaging and no extradural collection on spine MR imaging or conventional myelography. These patients underwent dynamic decubitus, positive-pressure CTM. Patients were classified as having either confirmed CVF (imaging and/or surgical diagnosis) or no definite etiology diagnosed for CSF leak.

CT Myelography Technique

All CTMs were performed by 2 experienced spinal neuroradiologists. A 22-ga Quincke spinal needle (BD) was placed under

intermittent CT fluoroscopy (Discovery CT 750; GE Healthcare) with the patient in the decubitus position. Intrathecal position was confirmed with a test dose of 0.5–1 mL of iohexol contrast (Omnipaque 300 mg; GE Healthcare). Opening CSF pressure was recorded using Glass-Tube (CareFusion) or a digital manometer (Compass; Centurion), allowing equilibration through several respiratory and cardiac cycles, typically 10–15 seconds (this approach was used both pre- and post-bolus infusion). Intrathecal pressure was recorded following serial infusions of normal saline in 1- to 5-mL boluses. When an inflection in CSF pressure (ie, a greater-than-expected change in pressure per bolus, shown in Fig 1) was observed, typically after 10–15 mL of infusion or positive-pressure augmentation was otherwise deemed adequate by the operator, CSF pressure was again recorded, and 8–10 mL of Omnipaque 300 mg was then instilled. Saline bolus infusion was also stopped if patients developed symptoms or peak CSF pressure approached 25–30 cm H₂O to avoid headache and acute visual changes, on the basis of empiric experience of an experienced spine neuroradiologist (unpublished data, W.P.D., May, 2020) and in consultation with a spine neurosurgeon. If the initial CTM was nondiagnostic, a subsequent CTM was performed with the patient in the opposite decubitus position on the following day. At our institution, decubitus dynamic CTM is performed using the HoverMatt device (HoverTech International), which allows rapid transient Trendelenburg positioning for approximately 10 seconds, which is then immediately reversed. Following this maneuver, diagnostic-dose CT is performed with the patient in the decubitus position (typically with 140 kV[peak] and 240 mA) in a dynamic caudal-cranial followed by cranial-caudal fashion, to optimally visualize signs of CVF.

CSF Compliance Analysis and Parameter Calculation

Serial CSF pressure and infusion volume recordings were plotted to generate CSC curves (Fig 1). The PVI was calculated for each patient according to the method of Marmarou et al.¹⁵ This method uses log-transformation of the exponential CSF compliance curve to simplify the calculation (Equation 1):

$$PVI = \frac{\Delta V}{\log_{10} \frac{P_p}{P_o}}$$

In this formula, ΔV is the incremental change in volume, equal to the normal saline bolus. P_p is the final (peak) pressure, and P_o is the initial pressure. The PVI value can then be used to estimate CSF-space compliance using an experimentally derived constant function for a given pressure.⁷ To estimate the compliance of the system in equilibrium, we calculated the compliance

Table 1: Demographic and CSF pressure-volume parameters for patients with clinical and imaging features of SIH, all of whom were suspected of having CVF^a

	Total (n = 22)	Definite or Probable CVF (n = 8)	No CVF Identified (n = 14)	P Value
Age (yr)	57.3	60.0	55.8	.5
Sex	59.1% F	37.5% F	71.4% F	.12
Increase in relative pressure during normal saline infusion (cm H ₂ O)	146.7% (SD, 17.3%)	148.5% (SD, 17.9%)	145.4% (SD, 27.0%)	.93
Total volume infusion (mL)	20.7 (SD, 1.8)	27.6 (SD, 2.9)	15.9 (SD, 4.1)	<.001
CSC curves with abrupt pressure loss	11/34 (32.4%)	4/14 (28.6%)	7/20 (35.0%)	.69
Opening pressure (cm H ₂ O)	11.6 (SD, 3.8)	9.8 (SD, 0.9)	12.8 (SD, 0.8)	.02
PVI ^b (mL H ₂ O)	63.9 (SD, 7.5)	77.5 (SD, 10.3)	54.3 (SD, 10.1)	.13
C _{op} ^c (mL/cm H ₂ O)	2.6 (SD, 0.3) mL/cm H ₂ O	3.8 (SD, 0.5) mL/cm H ₂ O	1.8 (SD, 0.3) mL/cm H ₂ O	<.001
Overall compliance (linear slope of CSC curve) (mL/cm H ₂ O)	2.0 (SD, 0.3)	3.1 (SD, 0.6)	1.3 (SD, 0.3)	.005

^a Eight patients had definite or probable CVF diagnosed on CTM, and the remaining cases (14/22) remain unconfirmed. All *P* values represent comparison of diagnosed-versus-undiagnosed groups. Data represent either proportions or mean values with standard deviation (SD).

^b Equation 1.

^c Equation 2.

at opening pressure using the following equation, assigning the value of *Pressure* as the measured opening pressure (Equation 2):

$$\text{Compliance} = \frac{0.4343 \times \text{PVI}}{\text{Pressure}}.$$

CSF-space compliance was also estimated as slope⁻¹ of the line of best fit estimated using linear regression of the pressure-volume curves (Fig 1A).¹⁶ Whereas Equation 2 defines the compliance at a particular pressure, the linear regression approximates the compliance over the range of pressures interrogated during saline infusion.

Statistical comparison of continuous variables between groups was assessed with Student *t* tests or the Mann-Whitney *U* test as appropriate. Frequency data were compared using the Pearson χ^2 test. *P* values < .05 were considered statistically significant. Statistical analyses were performed using R statistical and computing software (Version 3.6.2; <http://www.r-project.org/>).

RESULTS

Patient Characteristics

A total of 34 CTMs performed in 22 patients were included in the analysis (14 patients had a single CTM, 5 had 2 CTMs, 2 patients had 3 CTMs, and 1 patient had 4 CTMs). Patient demographic characteristics and a summary of CSC parameters by group are shown in Table 1. The mean age was 57.3 [SD, 13.7] years, and 59.1% of patients were women. Eight patients (36.4%) were diagnosed with confirmed CVF (4 by imaging and surgery, 4 by imaging alone), and the remaining 14 remained undiagnosed. There were no immediate postprocedural complications; however, 2 patients developed mild headaches during the injection (2/34 procedures, 5.8%), which resolved promptly during postprocedural observation.

The mean total normal saline bolus infusion volume was 20.7 [SD, 1.8] mL; range, 4–41 mL with significantly higher infusion volume in the confirmed CVF compared with the unconfirmed CVF group (*P* < .001). Mean opening pressure was lower in the confirmed CVF group (9.8 [SD, 0.9] versus 12.8 [SD, 0.8] cm

H₂O, *P* = .02). The average relative increase in CSF pressure from opening pressure baseline was 146.7% [SD, 17.3%] with no difference between the confirmed/unconfirmed CVF groups (148.5% [SD, 17.9%] versus 145.4% [SD, 27.0%], *P* = .93). The average peak CSF pressure after bolus augmentation was 26.3 [SD, 1.3] cm H₂O (interquartile range 16.3–36.3 cm H₂O). Peak CSF pressures were lower in the group with confirmed CVF, but the mean difference was not statistically significant (23.2 [SD, 2.1] versus 28.4 [SD, 1.6] cm H₂O, *P* = .06).

Craniospinal Compliance Parameters

The mean CSC parameters are summarized in Table 1. The mean PVI for all patients was 63.9 [SD, 7.5] mL. The mean PVI was higher in patients with confirmed CVF, but this difference was not statistically significant (PVI = 77.5 [SD, 10.3] versus 54.3 [SD, 10.1] mL/cm H₂O, *P* = .13). Patients with confirmed CVF had significantly higher compliance at opening pressure (C_{op}) (mean = 3.8 [SD, 0.5] mL/cm H₂O) than the unconfirmed CVF group (mean = 1.8 [SD, 0.3] mL/cm H₂O, *P* ≤ .001). The patient group with confirmed CVF also had higher overall compliance across the range of CSF pressure values compared with patients with unconfirmed CVF (mean = 3.1 [SD, 0.6] versus 1.3 [SD, 0.3] mL/cm H₂O, *P* = .005). Sex-related differences are shown in Table 2. No significant differences were observed between men and women for opening pressure, PVI, C_{op}, or overall compliance (*P* > .05, all cases).

CSC-Curve Morphology

We observed a spectrum of CSC curve shapes, including curves that were roughly linear, sigmoid, and exponential. We also found 2 distinct patterns that may have particular clinical relevance. A sudden drop in measured pressure during positive-pressure augmentation was observed in 11/34 (32.4%) patients (Fig 1). No difference in the frequency of this curve morphology was seen between the confirmed and unconfirmed CVF groups (28.6% versus 35.0%, *P* = .69). Continued administration of normal saline boluses after the pressure drop resulted in

Table 2: CSC parameter differences by sex^a

	Women	Men	P Value
Opening pressure (cm H ₂ O)	11.5 [SD, 0.8]	11.7 [SD, 1.0]	.86 ^b
PVI (mL H ₂ O)	57.5 [SD, 9.1]	74.1 [SD, 7.0]	.29 ^b
Compliance at opening pressure (mL/cm H ₂ O)	2.5 [SD, -0.5]	2.9 [SD, 0.4]	.06 ^c
Overall compliance (mL/cm H ₂ O)	1.7 [SD, 0.4]	2.5 [SD, 0.6]	.06 ^b

^a Data are mean values with standard deviation (SD).

^b Student *t* test.

^c Mann-Whitney *U* test.

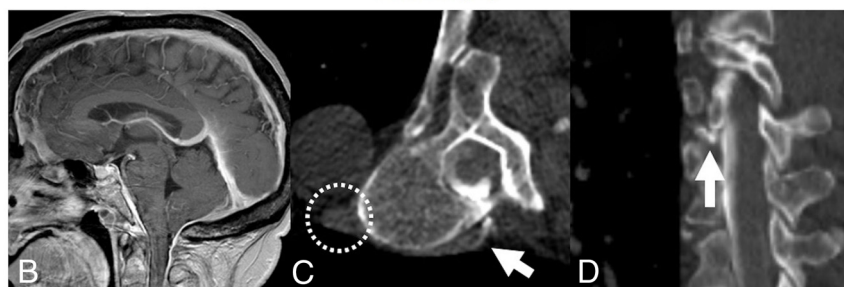
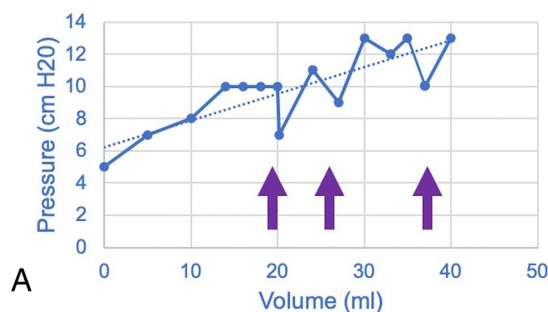


FIG 2. A craniospinal compliance curve in a 70-year-old woman with confirmed CVF (A) shows high compliance (ie, smaller change in pressure per increase in volume) with multiple abrupt pressure drops (arrows) above 10 cm H₂O. Recent brain MR imaging shows characteristic features of SIH (B), including reduced mamillopontine distance, low cerebellar tonsils, and pachymeningeal enhancement. A right T7–8 CVF was identified on decubitus CT myelography (C and D). Hyperdensity of the paraspinal vein and azygous vein (dashed circle) aids in identification of the fistula (white arrows). The patient was treated with percutaneous fibrin glue injection.

reconstitution of the CSC slope in each case, though multiple/recurrent drops were observed in some instances (Fig 2).

DISCUSSION

We report a method of generating craniospinal compliance curves derived from CT myelography and characterize these curves in a preliminary analysis of patients with SIH and suspected CVF. Compliance measurements (C_{op} , overall CSC compliance) in patients with confirmed CVFs were statistically different from those in patients with SIH in whom a final etiology of CSF leak could not be identified. Using a hand-bolus injection as a simple and reproducible alternative to continuous infusion techniques, we show how patient-specific models of pressure-volume dynamics can be reconstructed and the PVI can be estimated.

Although these findings are preliminary, we propose several potential uses of CSC curves in patients with SIH who undergo CTM: First, a drop in CSF pressure observed on the CSC curve may help identify patients with dural leaks or fistulas. Second, there

are probably pressure-dependent CVFs, that otherwise remain occult without adequate pressure augmentation (Fig 1). Finally, the documentation of CSF compliance may also define a patient-specific baseline, allowing quantification of treatment response, as we show with the epidural blood patch (Fig 3). For example, baseline patient-specific CSC parameters could be used in patients who undergo surgical fistula ligation as a means of confirming successful or unsuccessful CVF exclusion.

The theoretic basis for CSC curve analysis in patients with CSF leak warrants additional discussion. Abnormal profiles of PVI and the resistance to CSF outflow have been described in patients with intracranial pathology, including normal-pressure hydrocephalus, subarachnoid hemorrhage, and traumatic brain injury.^{17–19} However, contemporary models of CSF-space compliance treat the cranial and spinal spaces as communicating compartments of the same system.⁶ In these models, the CSC is analogized to an electrical circuit with systemic compliance determined by the additive effects of cranial and spinal compartments.^{16,13,20} Abnormal dural compliance in the spinal compartment should, therefore, influence the entire craniospinal system. CVF, like all spinal CSF leaks, should, in theory, increase compliance, but the pressure-volume relationship is likely dictated by the dynamic equilibrium of CSF pressure and venous pressure. Our

observation that in some patients, a sudden collapse of pressure occurred during saline infusion may indicate that we had reached a CSF-venous pressure equilibrium point. A further increase in CSF pressure could conceivably open the leak and provides one explanation for the inflection in compliance observed in this study (Fig 4). While unproven, this mechanism could provide a physiologic explanation for why CVFs are often occult in the supine position but manifest when the patient is upright or in the decubitus position or provocation maneuvers are performed. Our observation is also concordant with work from Amrhein et al,¹¹ which showed increased conspicuity of the CVF with inspiration, which augments the CSF-venous pressure gradient increasing venous return to the right atrium. It has been postulated that such maneuvers open the leak, which could be detected as a sudden increase in compliance of the craniospinal system.^{5,9,21} A similar mechanism was postulated by Kumar et al,²² who reported indirect treatment of CVFs by reduction of the CSF-venous gradient using an inferior vena cava stent.

The hand-injection bolus pressure augmentation method is easily reproducible and does not require additional equipment,

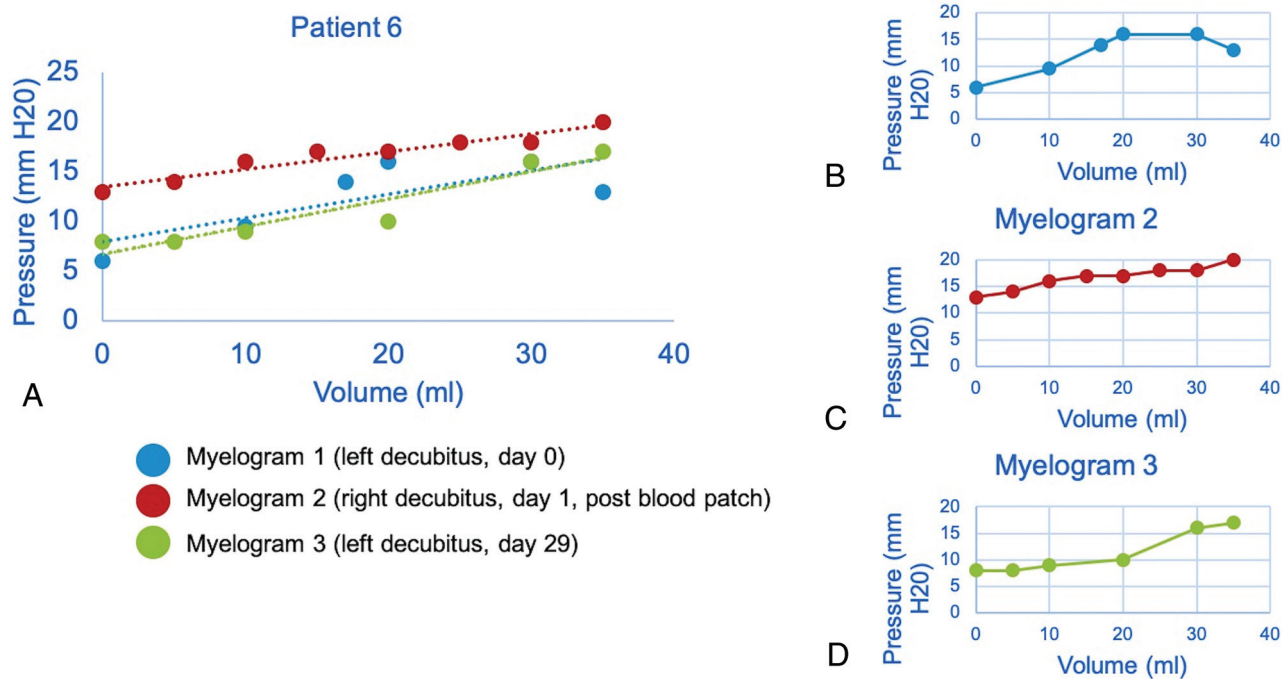


FIG 3. Craniospinal compliance curve in a 63-year-old woman suspected but not radiographically confirmed to have CVF. Estimated linear compliance for each CTM is shown as a *dashed line*, approximating the shape of the pressure-volume curve (A). The second CTM was performed after the blood patch showed an increase in opening pressure (B and C). The effect of the blood patch is diminished on delayed repeat CTM (D), in which the left side of the curve, including opening pressure, more closely matches the prepatch curve.

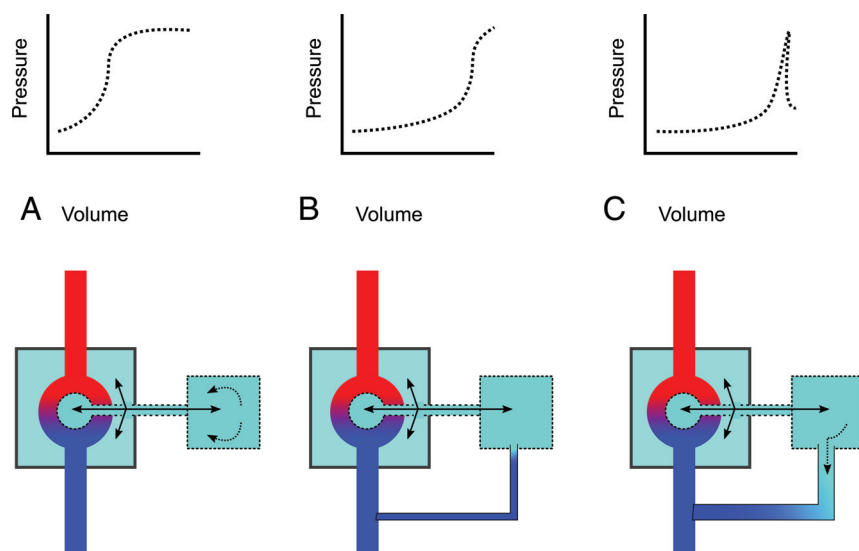


FIG 4. Schematic of the components of craniospinal compliance and hypothesized physiology of CVF (CSF = green, arterial blood = red, venous blood = blue). A normal CSC encompasses both intraventricular and subarachnoid CSF and is defined by cranial and spinal compartments (*larger and smaller boxes*, respectively) as well as the arteriovenous vascular bed (A). In dural tear CSF leak or CVF at low pressure, an equilibrium state (B) may exist in which the leak is occult by CTM. With special maneuvers (dynamic CTM, respiratory-phase variation, jugular pressure, and bolus-pressure augmentation), pressure gradients may open the leak, allowing detection on CTM (C).

described by Griffith et al²⁵ as a means of estimating compliance and PVI. This approach is based in mathematic and empiric observations showing that the PVI can be accurately measured using bolus (rather than steady/continuous) infusion.⁸ Although only a single bolus injection is needed to estimate PVI, multiple measurements, as used in our study, may be advantageous to identify zones in which the pressure-volume relationship changes more quickly due to autoregulatory mechanisms.²⁶ While dynamic CTM is the preferred technique at our institution, the bolus-pressure augmentation method could be performed with conventional or dynamic fluoroscopy. In this preliminary experience, we observed no peri-procedural complications and only 2 instances (5.8%) of transient headache during bolus infusion. These findings suggest that this technique has a reasonable safety profile when pressures and symptoms are closely monitored.

The interpretation of CSC curves has several important technical and theoretic limitations. First, because we did not investigate CSC parameters in controls without SIH, it is difficult to estimate the diagnostic value of CSC curves in

unlike previously described methods using steady-state infusion.^{20,23,24} The hand-bolus technique is more appropriate for patients with SIH than serial CSF withdrawal, which was

routine practice. A corollary limitation is that comparisons between confirmed and unconfirmed (suspected) CVFs are inherently limited and should be interpreted conservatively. Another important limitation is that CSC has been shown to vary with posture, largely due to shifts and redistribution of venous outflow through the jugular veins.²⁷ While our data suggest that a rapid drop in CSF pressure during pressure augmentation may reflect opening of a pressure-dependent CVF, this effect could plausibly be due to other physiologic effects such as respiratory phase variation and the cardiac cycle.¹¹ Definitive correlation could be established if the bolus-pressure augmentation technique were performed during digital subtraction myelography to allow real-time visualization of the CVF; we would expect that the leak would become visible or more conspicuous as CSF pressure is increased with serial intrathecal boluses, controlling for respiratory phase and cardiac cycle variations.

Another important limitation of our study is that the population included in this analysis comprised patients with suspected CVF who remained undiagnosed after conventional diagnostic and interventional studies (eg, MR myelography, conventional CTM). Accordingly, patients with other, non-CVF leaks are not represented, and the relatively low rate of confirmatory diagnosis (8/22, 36.4%) in this cohort reflects the diagnostic challenge of CVF relative to other forms of CSF leak.² Some of these patients may have leaks in locations that are more difficult to visualize (eg, sacrum) or simply CVFs that were not visible at that time. An additional important limitation of our study is that we did not assess control patients, and as a result, we did not define discriminatory threshold values of PVI and compliance in healthy patients. Nonetheless, the mean PVI values in our study (63.9 [SD, 7.5] mL) are higher than those in control patients reported in the literature, for example by Shapiro et al⁷ (PVI = 25.9 [SD, 3.7] mL) and by Wahlin et al¹³ (PVI mean = 9.8 [SD, 2.7 mL]), though methodologic differences may affect comparison. This finding is consistent with the proposed pathophysiology of CVF as a high-compliance state. A final limitation is that we did not use a standardized approach to positive-pressure augmentation because each operator selected the bolus number and volume before imaging.

This work is a preliminary exploration of a novel technique in a dynamic disease process; while these results are promising, investigation of CSC curves and correlation of steady-state and bolus-infusion methods should also be performed in the CSF leak population to confirm the validity of this approach. Future studies should also establish the boundaries of normal physiology in control patients.

CONCLUSIONS

This study describes a method of estimating craniospinal compliance during dynamic CT myelography and presents our preliminary experience in applying this technique in patients with suspected CVF. This method could be applied prospectively to evaluate compliance parameters and pressure-volume curve morphology as tools for the diagnosis of CVF and could inform the practice of spine interventionalists treating these patients.

Disclosures: Benjamin Laguna—OTHER RELATIONSHIPS: Cofounder of a pre-revenue company called Sira Medical (augmented reality).

REFERENCES

- Schievink WI, Moser FG, Maya MM. CSF-venous fistula in spontaneous intracranial hypotension. *Neurology* 2014;83:472–73 [CrossRef Medline](#)
- Kranz PG, Amrhein TJ, Gray L. CSF venous fistulas in spontaneous intracranial hypotension: imaging characteristics on dynamic and CT myelography. *AJR Am J Roentgenol* 2017;209:1360–66 [CrossRef Medline](#)
- Schievink WI. Spontaneous spinal cerebrospinal fluid leaks and intracranial hypotension. *JAMA* 2006;295:2286–96 [CrossRef Medline](#)
- Hunderfund ANL, Mokri B. Orthostatic headache without CSF leak. *Neurology* 2008;71:1902–06 [CrossRef Medline](#)
- Dobrocky T, Mosimann PJ, Zibold F, et al. Cryptogenic cerebrospinal fluid leaks in spontaneous intracranial hypotension: role of dynamic CT myelography. *Radiology* 2018;289:766–72 [CrossRef Medline](#)
- Burman R, Alperin N, Lee SH, et al. Patient-specific cranio-spinal compliance distribution using lumped-parameter model: its relation with ICP over a wide age range. *Fluids Barriers CNS* 2018;15:29 [CrossRef Medline](#)
- Shapiro K, Marmarou A, Shulman K. Characterization of clinical CSF dynamics and neural axis compliance using the pressure-volume index, I: the normal pressure-volume index. *Ann Neurol* 1980;7:508–14 [CrossRef Medline](#)
- Tans JT, Poortvliet DC. CSF outflow resistance and pressure-volume index determined by steady-state and bolus infusions. *Clin Neurol Neurosurg* 1985;87:159–65 [CrossRef Medline](#)
- Griffin AS, Lu L, Peacock S, et al. CSF volume provocation maneuvers during lumbar puncture as a possible predictive tool for diagnosing spontaneous intracranial hypotension. *Clin Neurol Neurosurg* 2019;186:105552 [CrossRef Medline](#)
- Kranz PG, Luetmer PH, Diehn FE, et al. Myelographic techniques for the detection of spinal CSF leaks in spontaneous intracranial hypotension. *AJR Am J Roentgenol* 2016;206:8–19 [CrossRef Medline](#)
- Amrhein TJ, Gray L, Malinzak MD, et al. Respiratory phase affects the conspicuity of CSF-venous fistulas in spontaneous intracranial hypotension. *AJNR Am J Neuroradiol* 2020;41:1754–56 [CrossRef Medline](#)
- Miller JD, Garibi J, Pickard JD. Induced changes of cerebrospinal fluid volume: effects during continuous monitoring of ventricular fluid pressure. *Arch Neurol* 1973;28:265–69 [CrossRef Medline](#)
- Wählin A, Ambarki K, Birgander R, et al. Assessment of craniospinal pressure-volume indices. *AJNR Am J Neuroradiol* 2010;31:1645–50 [CrossRef Medline](#)
- Qvarlander S, Lundkvist B, Koskinen L-OD, et al. Pulsatility in CSF dynamics: pathophysiology of idiopathic normal pressure hydrocephalus. *J Neurol Neurosurg Psychiatry* 2013;84:735–41 [CrossRef Medline](#)
- Marmarou A, Shulman K, LaMorgese J. Compartmental analysis of compliance and outflow resistance of the cerebrospinal fluid system. *J Neurosurg* 1975;43:523–34 [CrossRef Medline](#)
- Löfgren J, von EC, Zwetnow NN. The pressure-volume curve of the cerebrospinal fluid space in dogs. *Acta Neurol Scand* 1973;49:557–74 [CrossRef Medline](#)
- Pomschar A, Koerte I, Lee S, et al. MRI evidence for altered venous drainage and intracranial compliance in mild traumatic brain injury. *PLoS One* 2013;8:e55447 [CrossRef Medline](#)
- Eklund A, Smielewski P, Chambers I, et al. Assessment of cerebrospinal fluid outflow resistance. *Med Biol Eng Comput* 2007;45:719–35 [CrossRef Medline](#)
- Heinsoo M, Eelmäe J, Kuklane M, et al. The possible role of CSF hydrodynamic parameters following in management of SAH patients. In: Marmarou A, Bullock R, Avezaat C, et al, eds. *Intracranial Pressure and Neuromonitoring in Brain Injury*. Springer-Verlag; 1998:13–15
- Tain RW, Bagci AM, Lam BL, et al. Determination of cranio-spinal canal compliance distribution by MRI: methodology and early application in idiopathic intracranial hypertension. *J Magn Reson Imaging* 2011;34:1397–404 [CrossRef Medline](#)

21. Kranz PG, Gray L, Amrhein TJ. **Decubitus CT myelography for detecting subtle CSF leaks in spontaneous intracranial hypotension.** *AJNR Am J Neuroradiol* 2019;40:754–56 [CrossRef Medline](#)
22. Kumar N, Neidert NB, Diehn FE, et al. **A novel etiology for cranio-spinal hypovolemia: a case of inferior vena cava obstruction.** *J Neurosurg Spine* 2018;29:452–55 [CrossRef Medline](#)
23. Beck J, Fung C, Ulrich CT, et al. **Cerebrospinal fluid outflow resistance as a diagnostic marker of spontaneous cerebrospinal fluid leakage.** *J Neurosurg Spine* 2017;27:227–34 [CrossRef Medline](#)
24. Weerakkody RA, Czosnyka M, Schuhmann MU, et al. **Clinical assessment of cerebrospinal fluid dynamics in hydrocephalus: guide to interpretation based on observational study.** *Acta Neurol Scand* 2011;124:85–98 [CrossRef Medline](#)
25. Griffith B, Capobres T, Patel SC, et al. **CSF pressure change in relation to opening pressure and CSF volume removed.** *AJNR Am J Neuroradiol* 2018;39:1185–90 [CrossRef Medline](#)
26. Avezaat CJ, Eijndhoven JH, van Wyper DJ. **Cerebrospinal fluid pulse pressure and intracranial volume-pressure relationships.** *J Neurol Neurosurg Psychiatry* 1979;42:687–700 [CrossRef Medline](#)
27. Alperin N, Lee SH, Sivaramakrishnan A, et al. **Quantifying the effect of posture on intracranial physiology in humans by MRI flow studies.** *J Magn Reson Imaging* 2005;22:591–96 [CrossRef Medline](#)